ELSEVIER

Carbohydrate Research 264 (1994) 161–171

CARBOHYDRATE RESEARCH

Crystal structure and molecular mechanics analysis of methyl 6-*O*-(*N*-heptylcarbamoyl)-α-D-glucopyranoside (HECAMEG)

Søren Balling Engelsen [a], Serge Pérez [a,*], Loïc Toupet [b], Daniel Plusquellec [c]

[a] *Ingénierie Moléculaire, Institut National de la Recherche Agronomique, BP 527, 44026 Nantes, France*
[b] *Laboratoire Matière Condensée et Matériaux, C.N.R.S., Université de Rennes, Avenue du Général Leclerc, 35700 Rennes, France*
[c] *Laboratoire de Chimie Organique et des Substances Naturelles, C.N.R.S., Ecole Nationale Supérieure de Chimie de Rennes, Avenue du Général Leclerc, 35700 Rennes, France*

Received 13 April 1994; accepted 31 May 1994

Abstract

The crystal structure of methyl 6-*O*-(*N*-heptylcarbamoyl)-α-D-glucopyranoside (trivial name: HECAMEG), $C_{15}H_{29}NO_7$, was determined using Mo*Kα* X-ray data at 110 K. The space group is $P2_12_12_1$, with four molecules in a unit cell having dimensions of $a=5.070$ (5), $b=8.282$ (4), and $c=43.16$ (2) Å. Because all the crystals which could be grown were twinned, a high-resolution data set could not be collected. Consequently, a highly refined structure could not be reached. Therefore, the crystalline structure was submitted to a further refinement based on optimization of both intramolecular and intermolecular interactions using molecular mechanics methods. The present work provides structural information about the fairly uncommon carbamoyl group, as well as on the amphiphilic components of HECAMEG. A $^4C_1$ conformation is maintained for the glucopyranoside, and the orientation around C-5–C-6 is *gauche–gauche*; the polymethylene chain is observed in its fully extended, all *anti* conformation. Whereas there is no intramolecular hydrogen bonding, three intermolecular H bonds are observed. One involves the N–H of the carbamoyl group linked to the carbonyl oxygen of a neighboring group. The two others link the secondary hydroxyl groups of the glucopyranose through a network which propagates along one of the 2_1 screw axis. A complete analysis of the intermolecular arrangement has been performed, which yields a detailed analysis of the crystal packing. To the best of our knowledge this is the first amphiphilic carbohydrate structure which crystallizes in a bilayer type of arrangement not having interdigitized hydrophobic acyl chains.

* Corresponding author.

SSDI 0008-6215(94)00201-P

Keywords: X-ray crystallography; Methyl 6-*O*-(*N*-heptylcarbamoyl)-α-D-glucopyranoside; Surfactant; Molecular mechanics

1. Introduction

The emergence of new biological and biomedical applications for surfactants has emphasized the need for highly purified compounds. In membrane studies, surfactants are required for the solubilization and purification of amphiphilic membrane proteins in the perspective of their structural and functional characterization [1]. Surfactants have also proved to be useful in virucidal treatment of plasma derivatives and particular for the inactivation of lipid-coated viruses [2].

Among the numerous surfactants at present available, synthetic glycolipids proved to be the most useful, particularly when retention of the biological activity is of importance [1]. In this field, methyl 6-*O*-(*N*-heptylcarbamoyl)α-D-glucopyranoside (HECAMEG) is emerging as a powerful surfactant in comparison with other ones sharing similar properties [3,4]. The usefulness of HECAMEG for membrane studies was ascertained by its ability to extract membrane proteins with selectivity, an operation very useful for their purification, and by its mildness toward structure and function of amphiphilic and soluble enzymes [3]. Moreover, HECAMEG has recently been reported to inhibit the herpes simplex virus II in protein-containing solutions without interfering with the active blood components [5]. In order to characterize some of the unique features that the HECAMEG (**1**) glycolipid may exhibit, we have undertaken the elucidation of its molecular and crystalline structure through the combined use of X-ray diffraction and molecular mechanics calculations.

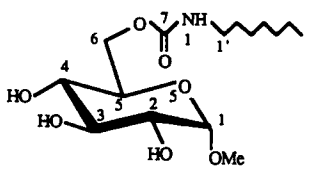

2. Experimental

Nomenclature.—The recommendation and symbols proposed by the Joint Commission on Biochemical Nomenclature are used throughout this paper [6].

Crystal growth and morphology.—Crystals of HECAMEG were grown from 1:3 CH_2Cl_2–diisopropyl ether, but most were either too thin for X-ray investigation or were twinned.

Crystal structure resolution.—A single crystal of dimensions $0.15 \times 0.25 \times 0.45$ mm was used. The unit-cell dimensions were obtained as part of the crystal alignment on a CAD4 Enraf–Nonius diffractometer by a least-squares fit to the setting of well-centred reflections having high 2θ values. The unit-cell parameters and crystallographic data of interest are given in Table 1.

The intensities of 1926 independent reflections were measured on a four-circle diffractometer inside the sphere limited by $2\theta \leq 50°$ at the Mo$K\alpha$ wavelength using the $\omega - 2\theta$

Table 1
Crystal data and structure determination and refinement data for methyl 6-*O*-(*N*-heptylcarbamoyl)-α-D-glucopyranoside

Molecular formula	$C_{15}H_{29}NO_7$
Molar mass	335.40 g
Crystal system	Orthorhombic
Space group	$P2_12_12_1$
Z	4
a	5.070 (5) Å
b	8.282 (4) Å
c	43.16 (2) Å
V	1812 (2) Å^3
D_c	1.229 g/cm^3
Crystal size	$0.15 \times 0.25 \times 0.45$ mm^3
$F(000)$	728
μ (Mo$K\alpha$)	0.91
T	110 K

technique. The average of the reference reflections monitored each hour decreased by 1.5% over the duration of the data collection. All the intensities were corrected from the background noise. From 1926 measured reflections, 991 such as $I/\sigma(I) \geq 1.5\sigma$ were considered as observed. Lorentz and polarization corrections were applied. Due to the small size of the crystal investigated and the small value of its absorption coefficient at the wavelength used, no absorption correction was applied. Scattering factors were taken from the International Tables of Crystallography [7]. The structure was solved by direct methods [8,9], allowing the location of all C, O, and N atoms. Some of the H atoms were located by successive difference Fourier maps and isotropic refinement, leading to an R value of 0.16. The last refinement cycles were performed using an anistropic thermal temperature factor. The final R value was 0.098. During the refinement, each reflection was assigned a weight $w = [\sigma^2(I) + (0.04\, F_o^2)^2]^{-1/2}$ derived from $\sigma(I)$. A final electron density map showed no significant residual density, the extreme fluctuations being 0.38 e Å^{-3}. The complete structural elucidation and refinement were performed using the MolEN suite of programs [10].

Molecular mechanics calculations.—Two molecular modeling programs were used, MM3(92) [11,12] and the Tripos force-field [13,14] with a modified set of parameters (PIM) [15] specifically for carbohydrates and implemented in the SYBYL molecular modeling package [13]. MM3 uses terms for van der Waals forces, electrostatic dipole interactions, hydrogen bonding, and special corrections for anomeric effects. A pseudo-Morse potential is used for bond stretching, a fourth-order potential for angle bending, and a Fourier series for modeling torsional energy. Cross-terms for torsion–stretch, torsion–bend, and bend–bend interactions are included. A dielectric constant of 4 was used throughout all the calculations [16]. The energy optimization continued until the energy changed by less than $n \cdot 0.00008$ kcal/mol, where n is the number of atoms in the molecule. The Tripos force-field is based on a set of classic molecular mechanics potential energy functions, including harmonic terms for bond stretching, angle bending, and out-of-plane bending, a torsional term, Lennard–Jones type nonbonded interactions, and a coulombic term between partial charges. Hydrogen bonding energy is taken into account in the following way: the

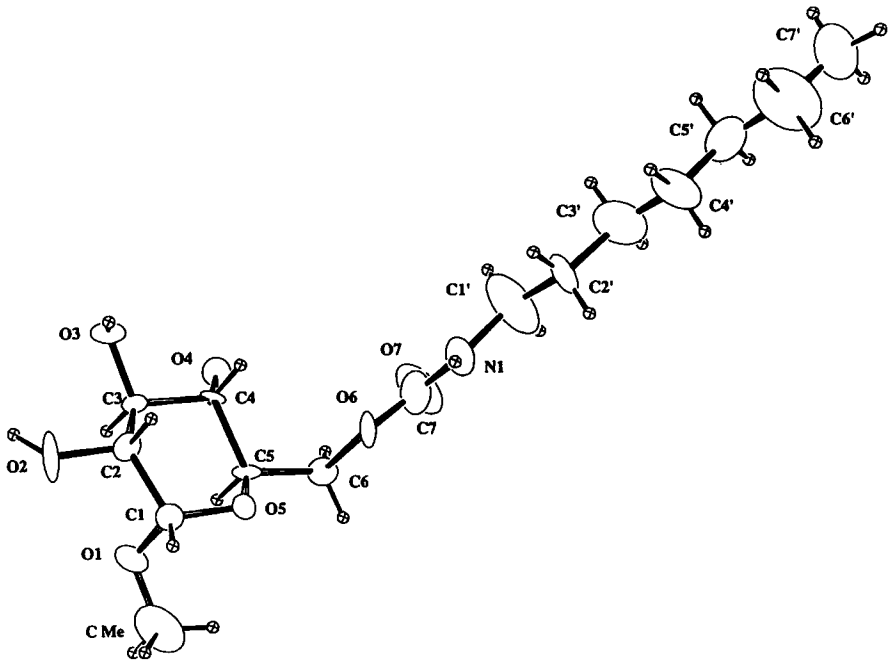

Fig. 1. Three-dimensional representation of the molecule of HECAMEG in the crystal, along with the atom labeling. Thermal ellipsoids are drawn at 50% probability

Van der Waals interactions between donor and acceptor, and hydrogen atoms linked to the donor are omitted. Only favorable electrostatic interactions between these atoms are computed. The atomic charges are derived from the semiempirical program MNDO [17]. Appropriate parameters for carbohydrates (PIM) which take into account for such stereoelectronic effects as the anomeric and exo-anomeric effect have been derived [15].

In order to arrive at a full description of the packing arrangement, the intermolecular energy between a given molecule, i.e., the reference molecule and all its neighbors, were evaluated by taking into account the intermolecular nonbonded interactions, including the hydrogen bonds. These calculations were performed using the same molecular mechanics program as those utilized in the conformational analysis of a single molecule. In addition, the number of "close" contacts corresponding to interatomic distances less than 1.5 times the sum of Van der Waals radii of the interacting atoms have been evaluated.

Miscellaneous.—The crystal structure computations were carried out on a MicroVax 31 000, whereas all the molecular mechanics calculations were run on RISC 6000 IBM and Silicon Graphics workstations.

3. Results and discussion

The molecular conformation of HECAMEG is shown in Fig. 1, together with the atom labelling and the 50% probability thermal ellipsoids [1]. The final atomic coordinates derived

[1] Observed and calculated positional parameters have been deposited with the Cambridge Crystallographic Data Centre and may be obtained upon request from the Director, CCDC, 12 Union Road, Cambridge CB2 1EZ, UK.

from X-ray refinement are listed in Table 2. A tabulation of the observed and calculated structure factors are available as supplementary material filed with the CCDC. The accuracy of the structural determination has been considerably hampered by the lack of availability of good crystals. Realizing the limited resolution of the crystal structure at the intramolecular level, an optimized structure of HECAMEG was calculated using the standard energy minimization algorithm in the MM3 force field. The content of the carbamoyl functional group made it necessary to constrain some torsional angles to the measured values due to the lack of parameters in MM3 for the following internal coordinates: N-1–C-7–O-6, N-1–C-7–O-6–C-6, O-6–C-7–N-1–C-1′, and O-6–C-7–N-1–HN1, all related to the neighboring amido and carboxyl groups. Also the three mobile exocyclic hydroxyl groups were constrained in order to conserve their orientations in the crystal. The impact of these constraints is not considered of major importance since they mostly concern the configuration about the fairly rigid and highly planar peptide bond. The coordinates of all nonhydrogen atoms were least-squares fitted to the original crystal structure and converted back to fractional coordinates using the inverse transformation matrix. The idealized MM3 coordinates are listed in Table 2 together with the measured crystal coordinates. The resulting rms difference in cartesian space based on all nonhydrogen atoms was calculated to be 0.0525 Å. Thus, MM3 was fairly neutral to the overall shape of the molecule as can be seen from Table 3, which lists the torsional angles of interest. The difference in the dihedral structure is hardly significant; however, all abnormal bond lengths and valence angles are corrected. As an example, the range of standard aliphatic C–C bond lengths which in the X-ray structure was from 1.346 to 1.564 Å has been considerably narrowed in the idealized structure ranging from 1.521 to 1.537 Å. Similar deviations are seen for other internal coordinates.

The present structural elucidation establishes that HECAMEG is a multifunctional amphiphilic mesogen with a hydrophilic hydrogen bonding carbohydrate moiety to which a hydrophobic aliphatic side chain is attached at the O-6 position, linked together by a carbamoyl group. As in all other crystal structures of hexopyranoses, HECAMEG is found to possess a $^4C_1$ chair conformation, though slightly deformed. The O-5–C-1–O-1–CMe torsional angle is observed to be $+65°$, indicating that the exo-anomeric effect is operative. The substituted primary hydroxyl group is found to be almost perfectly staggered ($-63°$) in the *gauche–gauche* conformation. Only the following relatively flexible C-5–C-6–O-6–C-7 torsional angle is distorted ($-142°$), probably due to an optimization of the angle orientation of the acyl chain with respect to the sugar ring within the packing. The peptide C-7–N-1 bond has a partial double-bond character; it is observed to be in the *trans* conformation as in all other similar crystal structures. The torsional angle about the N-1–C-1′ bond, which does not have the double-bond character, is found to be $-172°$. The polymethylene chain is observed in its fully extended all-*anti* conformation as always seen for aliphatic hydrocarbon chains in crystal structures [18].

There is no intramolecular hydrogen bonding, and only three different intermolecular hydrogen bonds are observed, the characteristics of which are listed in Table 4. The first hydrogen bond involves the N–H of a carbamoyl group with the carbonyl oxygen atom of a neighboring group in the *a* direction. Another network involves the three secondary hydroxyl groups of the glucopyranoside moiety through the establishment of two hydrogen bonds; O-2 acts both as a donor and as an acceptor, whereas O-3 donates one, and O-4

Table 2
Crystal coordinates and their estimated standard deviations and their equivalent temperature factors as derived from refinement of the structure and as derived from molecular mechanics optimization of the unit cell content

Atom	*X/a*	*Y/b*	*Z/c*	B(A^2) [a]	*X/a*	*Y/b*	*Z/c*
C-1	0.320 (2)	0.099 (1)	0.1939 (4)	2.0 (7)	0.3171	0.0992	0.1940
C-2	0.339 (2)	0.208 (1)	0.2217 (3)	1.9 (2)	0.3536	0.2155	0.2210
C-3	0.120 (2)	0.327 (2)	0.2247 (4)	1.6 (2)	0.1162	0.3268	0.2250
C-4	0.066 (2)	0.416 (1)	0.1942 (3)	1.8 (2)	0.0625	0.4116	0.1942
C-5	0.034 (2)	0.287 (1)	0.1680 (3)	1.6 (2)	0.0253	0.2851	0.1687
C-6	−0.015 (3)	0.363 (2)	0.1368 (3)	3.2 (3)	−0.0240	0.3599	0.1369
C-7	0.119 (4)	0.606 (2)	0.1143 (4)	4.5 (4)	0.1224	0.6056	0.1133
C-1′	0.304 (3)	0.864 (2)	0.0932 (5)	7.4 (5)	0.2881	0.8622	0.0937
C-2′	0.517 (3)	0.942 (2)	0.0821 (4)	3.6 (3)	0.5458	0.9398	0.0835
C-3′	0.514 (4)	1.106 (2)	0.0679 (5)	6.4 (5)	0.5036	1.1062	0.0688
C-4′	0.742 (4)	1.186 (2)	0.0566 (4)	5.6 (4)	0.7626	1.1834	0.0577
C-5′	0.725 (4)	1.344 (2)	0.0443 (4)	5.3 (4)	0.7201	1.3519	0.0437
C-6′	0.967 (5)	1.431 (2)	0.0328 (6)	9.3 (7)	0.9783	1.4282	0.0321
C-7′	0.934 (5)	1.587 (3)	0.0200 (5)	7.7 (6)	0.9361	1.5971	0.0184
C-Me	0.072 (5)	−0.128 (2)	0.1771 (4)	7.8 (5)	0.0755	−0.1303	0.1766
N-1	0.335 (2)	0.696 (1)	0.1063 (3)	3.1 (2)	0.3255	0.7045	0.1081
O-1	0.104 (2)	−0.006 (1)	0.2000 (2)	4.1 (3)	0.1047	−0.0087	0.2000
O-2	0.376 (2)	0.118 (1)	0.2495 (2)	3.4 (2)	0.3970	0.1203	0.2485
O-3	0.174 (2)	0.4489 (9)	0.2472 (2)	2.6 (2)	0.1731	0.4478	0.2480
O-4	−0.167 (2)	0.502 (1)	0.1953 (2)	2.8 (2)	−0.1743	0.5057	0.1977
O-5	0.270 (2)	0.1888 (9)	0.1661 (2)	2.3 (2)	0.2616	0.1892	0.1666
O-6	0.203 (2)	0.471 (1)	0.1288 (2)	2.9 (2)	0.1895	0.4675	0.1286
O-7	−0.104 (2)	0.647 (1)	0.1096 (3)	5.9 (3)	−0.1113	0.6353	0.1053
H-1	0.47	0.03	0.189	4*	0.5032	0.0295	0.1906
H-2	0.51	0.27	0.218	4*	0.5330	0.2891	0.2164
H-3	−0.04	0.26	0.230	4*	−0.0602	0.2564	0.2322
H-4	0.21	0.49	0.190	4*	0.2296	0.4930	0.1884
H-5	−0.12	0.21	0.174	4*	−0.1460	0.2058	0.1744
H-61	−0.18	0.43	0.137	4*	−0.2158	0.4235	0.1373
H-62	−0.05	0.28	0.120	4*	−0.0395	0.2638	0.1192
H-11′	0.16	0.85	0.075	4*	0.1574	0.8519	0.0731
H-12′	0.19	0.93	0.107	4*	0.1868	0.9451	0.1101
H-21′	0.64	0.94	0.100	4*	0.6798	0.9519	0.1039
H-22′	0.60	0.87	0.067	4*	0.6470	0.8591	0.0666
H-31′	0.38	1.11	0.052	4*	0.3658	1.0949	0.0488
H-32′	0.44	1.18	0.085	4*	0.4069	1.1876	0.0860
H-41′	0.88	1.18	0.073	4*	0.9024	1.1926	0.0776
H-42′	0.81	1.11	0.040	4*	0.8572	1.1033	0.0402
H-51′	0.59	1.35	0.028	4*	0.5782	1.3431	0.0240
H-52′	0.65	1.42	0.061	4*	0.6282	1.4324	0.0613
H-61′	1.10	1.43	0.050	4*	1.1216	1.4362	0.0517
H-62′	1.05	1.35	0.018	4*	1.0695	1.3487	0.0143
H-71′	1.11	1.63	0.011	4*	1.1249	1.6502	0.0101
H-72′	0.87	1.66	0.033	4*	0.8522	1.6818	0.0358
H-73′	0.82	1.59	0.001	4*	0.7983	1.5941	−0.0017
HN-1	0.51	0.66	0.111	4*	0.5088	0.6697	0.1159
HO-2	0.26	0.14	0.267	4*	0.2823	0.1562	0.2644

Table 2 (continued)

Atom	X/a	Y/b	Z/c	B(A^2) [a]	X/a	Y/b	Z/c
HO-3	0.39	0.45	0.249	4*	0.3573	0.4535	0.2515
HO-4	−0.39	0.46	0.191	4*	−0.3241	0.4409	0.1935
HMe-1	0.05	−0.08	0.156	4*	0.0328	−0.0753	0.1536
HMe-2	−0.09	−0.19	0.182	4*	−0.0916	−0.2105	0.1828
HMe-3	0.23	−0.20	0.181	4*	0.2573	−0.2053	0.1749

[a] $B(A^2) = (4/3)*[a^2*B(1,1) + b^2*B(2,2) + c^2*B(3,3) + ab(\cos\gamma)*B(1,2) + ac(\cos\beta)*B(1,3) + bc(\cos\alpha)*B(2,3)]$.

accepts one. This results in a propagation along the 2_1 screw axis running parallel to the *b* crystal axis.

a-direction: O-7···HN-1–N-1–C-7=O-7···HN-1

O-2···HO-3–O-3

b-direction: HO-2···O-4–C-4–C-3–C-2–O-2–HO-2···O-4

HO-3

The crystalline arrangement of HECAMEG is shown in Fig. 2. The packing can be described as a head-to-head bilayer, typical for monosubstituted acylated sugars [18]. The stacking of the bilayers is done by a unique highly angled terrace type of interaction not very different from that of the triglycerides [19,20] and that of the double chained sphingolipids [21]. The acyl chains are not interdigitizing as exclusively observed for carbohydrate amphiphilic structures which crystallize in a bilayer arrangement. This atypical bilayer stacking may be induced by the C=O···H–N hydrogen bond; it can be regarded as a compromise between the more favorable interdigitizing arrangement and an optimization of the hydrogen bond. Within the bilayer structure the hydrophobic acyl chains are stacked into hexagonal arranged columns, tilted 64° with respect to the normal of the bilayer plane, resulting in a very small bilayer thickness of 21.6 Å. The aforementioned unique features result from a particularly weak crystalline arrangement along the *c*-axis.

The molecular packing into a crystal lattice is generally believed to be directed by an optimization of the intermolecular dispersion attraction and the intermolecular electrostatic attraction. Hydrogen bonds are a mixture of these attractive forces, though mainly of electrostatic character. In order to investigate the anisotropy of the packing, we calculated the dimerization energies to all the close neighbors in the lattice using two different molecular mechanics force fields, PIM and MM3 (Table 5). The neighboring molecules are given an identification code which uses the combinations of the symmetry operation of the space group and the translational symmetry operations. Both model interatomic interactions by an effective pairpotential, and both neglect the atomic anisotropy of the dispersion and short-range repulsive interactions. The results, especially those obtained using MM3, do not seem to obey the general acceptance that the energy of a hydrogen bond lies in the range 3–8 kcal/mol [22,23]. The resulting dimerization energies using PIM indicates that the

Table 3
Torsional angles (deg) of interest for HECAMEG

Torsion	X-ray	MM3
Ring conformation		
O-5–C-1–C-2–C-3	48.9	55.2
C-1–C-2–C-3–C-4	−47.8	−54.1
C-2–C-3–C-4–C-5	51.0	55.7
C-3–C-4–C-5–O-5	−58.0	−59.5
C-4–C-5–O-5–C-1	62.4	63.3
C-5–O-5–C-1–C-2	−56.6	−60.4
Exocyclic torsions		
C-5–O-5–C-1–O-1	60.0	60.4
O-5–C-1–O-1–CMe	65.1	65.0 [a]
O-1–C-1–C-2–O-2	58.2	57.2
O-2–C-2–C-3–O-3	64.4	67.3
O-3–C-3–C-4–O-4	−68.4	−65.2
O-4–C-4–C-5–C-6	60.6	62.8
O-5–C-5–C-6–O-6	−63.1	−63.0 [a]
C-4–C-5–C-6–O-6	58.5	56.9
Carbamoyl group + aliphatic chain		
C-5–C-6–O-6–C-7	−141.7	−142.0 [a]
C-6–O-6–C-7–O-7	5.1	−3.6
C-6–O-6–C-7–N-1	−177.0	175.8
O-7–C-7–N-1–C-1′	5.1	3.1
O-6–C-7–N-1–C-1′	−172.4	−176.2
C-7–N-1–C-1′–C-2′	−172.1	−167.5
N-1–C-1′–C-2′–C-3′	178.5	−179.2
C-1′–C-2′–C-3′–C-4′	179.5	−178.5
C-2′–C-3′–C-4′–C-5′	−178.0	−178.8
C-3′–C-4′–C-5′–C-6′	178.8	−179.2
C-4′–C-5′–C-6′–C-7′	178.3	−179.4

([a] Dihedral angle was constrained during energy minimization.

optimal packing modes are obtained by pure translation in the a and b directions, and that the dispersion attraction is the major stabilizing intermolecular force. It also indicates that the stacking of the bilayers in the c direction without interdigitizing aliphatic chains is less favourable, but apparently the angled terrace type stacking (IV + 2b) is relatively profitable, especially when compared to the small contact hydrogen-bonding dimers (III + b and

Table 4
Packing features and hydrogen bonding [a]

D–H···A	Symmetry operation [b]	r (D···A)	r (H···A)	∠ (D–H···A)
N-1···O-7	I + a	2.877	1.947	157.8
O-2···O-4	III-b	2.779	2.044	128.2
O-3···O-2	III + a	2.681	1.840	128.6

[a] Bond lengths are in Å and angles are in degrees.
[b] Symmetry operations: I, (x, y, z); II, $(-x+1/2, -y, z+1/2)$; III, $(-x, y+1/2, -z+1/2)$; IV, $(x+1/2, -y+1/2, -z)$.

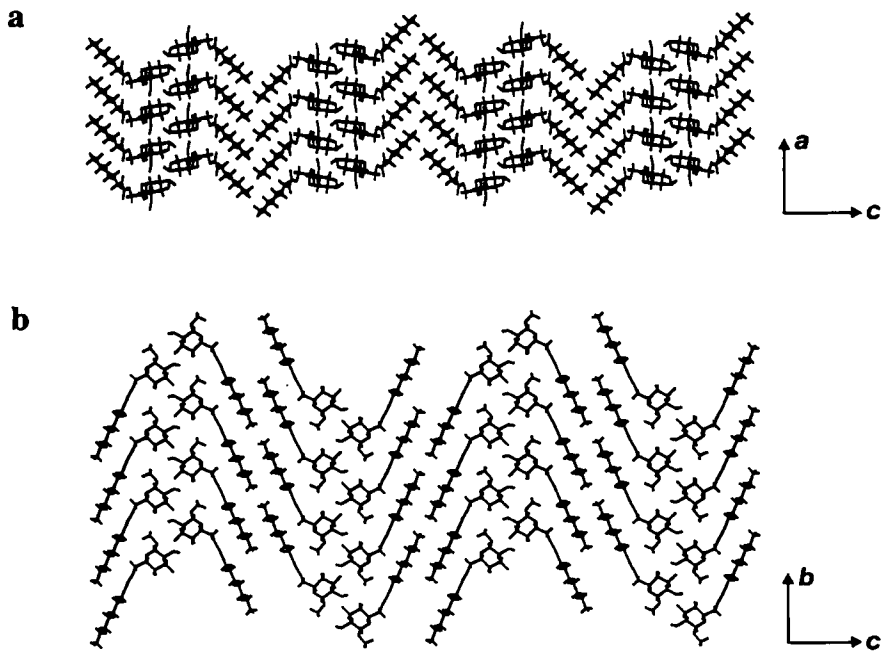

Fig. 2. Packing features of the molecule of HECAMEG in its unit cell. (a) View of the a–c plane orthogonal to the b-axis and (b) view of the b–c plane orthogonal to the a-axis.

III$+a-b$). Generally the PIM dimerization energies support the lattice data with the strongest interaction being in the shortest a direction and the second strongest interaction being in the second shortest lattice direction b. It is interesting to note that when adding the (III$-b$) dimerization energy, which acts purely in the b direction, to the (I$+b$) dimeri-

Table 5
Packing features and dimerization energies

Symmetry operations [a]	Close contacts (HB) [b]	E_{dim} (MM3) [c]	E_{dim} (PIM) [c]
I$+a$	191 (1)	−4.6	−11.0
I$-a$	191 (1)	−4.6	−11.0
I$+b$	102 (0)	−4.8	−8.1
I$-b$	102 (0)	−4.8	−8.1
I$+a+b$	70 (0)	−3.5	−5.4
I$-a-b$	70 (0)	−3.5	−5.4
IV$-a+2b$	51 (0)	−2.1	−3.8
IV$+2b$	51 (0)	−2.1	−3.8
III$-b$	59 (1)	−2.1	−3.7
III	59 (1)	−2.1	−3.7
III$+a-b$	32 (1)	−2.7	−2.6
III$+a$	32 (1)	−2.7	−2.6

[a] Symmetry operations: I,(x,y,z); II, ($-x+1/2,-y,z+1/2$); III, ($-x,y+1/2,-z+1/2$); IV, ($x+1/2,-y+1/2,-z$).
[b] Close contacts are all intermolecular distances less than 1.5 times the sum of the atomic Van der Waals radii.
[c] Energies are in kcal/mol.

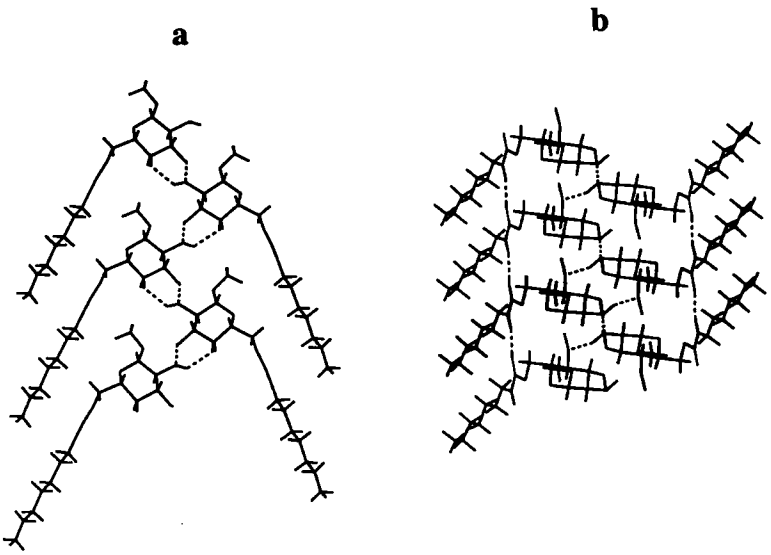

Fig. 3. Details of the anisotropy of packing of HECAMEG. (a) The *b*-directional head-to-head packing and (b) the *a*-directional head-to-head packing. Hydrogen bonds are shown as dashed lines.

zation energy we obtain approximately the same energy as that for the pure *a* translation (I+*a*), indicating almost isotropic bilayer directions. Considering these data it is easy to imagine the *a*-directional translation chain (Fig. 3a) serving as nucleation center for the crystal growth stabilized by the dynamically stable C=O···H–N hydrogen bond, quickly growing in the *b* direction to form a bilayer structure (Fig. 3b).

The molecular arrangement found in the crystal structure packing displays a very strong anisotropy: some intermolecular interactions are very strong; others are extremely weak. This is reflected by the magnitude of the crystalline density of 1.24 g/cm^3. The packing density as expressed by the Kitaigorodskii coefficient [24] is calculated to 0.69, indicating neither a very loose packing nor a very dense one. The difficulties for the molecules to grow in pure crystal lattices has, in our opinion, to be found in the mode of bilayer stacking.

4. Conclusions

Besides its possible commercial use as a detergent, HECAMEG is an ideal model in which to study molecular packing mechanisms and energetics. In the crystalline state it is presumably fairly rigid, having only the three secondary hydroxyl groups and the tilt angle mainly defined by the flexible C-6–O-6–C-7–N-1 torsion as internal degrees of freedom. The limited number of internal degrees of freedom and the fact that it grows as twin crystals makes HECAMEG a doable and very interesting model compound for theoretical investigation of possible modes of packing. In the liquid bilayer state where the molecules rearrange into a more relaxed and less symmetric two dimensional array, CP-MAS NMR spectroscopy has the potential to reveal changes in layer thickness, tilt angle and interaction modes. Finally, the capability of HECAMEG to form micelles gives the possibility to discover yet another

important packing feature of this extraordinary molecule as it has already served as a model compound for investigation of micelle-formation kinetics [4].

The reason why HECAMEG exhibits a high efficiency and selectivity for the extraction of surface mycoplasma antigens has not yet been elucidated [3]. However, the molecular arrangement found in the crystal structure suggests that the interactions of this surfactant with both biomembranes and proteins could be different from that of other synthetic compounds, e.g., octyl β-D-glucopyranoside. In addition to its strong hydrophobic interactions with the membrane-anchoring domain, one may speculate, *inter alia*, that HECAMEG might disrupt the interactions of the protein with the outer leaflet membrane glycolipids by establishing strong hydrogen bonds with the polypeptides through the carbamoyl linkage.

Acknowledgements

We thank W. Klagba (Vegatec, Villejuif, France) for a gift of HECAMEG.

References

[1] W. Kühlbrandt, *Quat. Rev. Biophys.*, 25 (1992) 1–49, and references therein.
[2] P. Hellstern, H. Sachse, H. Schwinn, and K. Oberfrank, *Vox. Sang.*, 63 (1992) 178–185.
[3] D. Plusquellec, G. Chevalier, R. Talibart, and H. Wroblewski, *Anal. Biochem.*, 179 (1989) 145–153.
[4] M. Frindini, B. Michels, and R. Zana, *J. Phys. Chem.*, 96 (1992), 8137–8141.
[5] R. Schmitthaeusler, W. Klagba, and F. Le Goffic, Fr. Pat. 267 4536; *Chem. Abstr.*, 118 (1992), 32924a.
[6] IUPAC-IUB Commision on Biochemical Nomenclature, *Arch. Biochem. Biophys.*, 145 (1971) 405–421.
[7] International Tables for X-ray Crystallography, Vol. IV, Kynoch Press, UK, 1974, pp 282–288 (now distributed by Kluwer Academic Press, Dordrecht).
[8] G.M. Sheldrick, SHELX76, Program for Crystal Structure Determination, University of Cambridge, UK, 1976.
[9] G.M. Sheldrick, SHELXS86, Program for the Solution of Crystal Structures, University of Göttingen, Federal Republic of Germany, 1986.
[10] C.K. Fair, MolEN, An Interactive Intelligent System for Crystal Structures Analysis, Enraf–Nonius, Delft, Netherlands, 1990.
[11] N.L. Allinger, Y.H. Yuh, and J.-H. Lii, *J. Am. Chem. Soc.*, 111 (1989) 8551–8566.
[12] N.L. Allinger, M. Rahman, and J.-H. Lii, *J. Am. Chem. Soc.*, 112 (1990) 8293–8307.
[13] Tripos Associates, 1699 S. Hanley Road, Suite 303, St. Louis, MO 63144 (USA). SYBYL 5.2, 1988.
[14] M. Clark, R.D. Cramer III, and N. van Opendosch, *J. Comput. Chem.*, 10 (1989) 982–1012.
[15] A. Imberty, K.D. Hardman, J.P. Carver, and S. Pérez, *Glycobiology*, 1 (1991) 631–642.
[16] A.D. French, R.J. Rowland, and N.L. Allinger, *ACS Symp. Ser.*, 430 (1990) 120–140.
[17] M.J.S. Dewar and W. Thiel, *J. Am. Chem. Soc.*, 99 (1977) 4899–4907. MNDO is an integrated part of the MOPAC 5.0 program (QCPE program No. 455).
[18] G.A. Jeffrey and L.M. Wingert, *Liq. Cryst.* 12 (1992) 179–202.
[19] K. Larsson, *Arkiv Kemi*, 23(1) (1964) 1–15.
[20] L.H. Jensen and A.J. Mabis, *Acta Crystallogr.*, 21 (1966) 770–781.
[21] I. Pascher, M. Lundmark, P.-G. Nyholm, and S. Sundell, *Biochim. Biophys. Acta*, 1113 (1992) 339–373, and references therein.
[22] M. Rigby, E.B. Smith, W.A. Wakeham, and G.C. Maitland, *The Forces Between Molecules*, Oxford University Press, Walton Street, Oxford OX2 6DP, UK, 1986.
[23] G.A. Jeffrey and W. Saenger, *Hydrogen Bonding in Biological Structures*, Springer-Verlag, Berlin, 1991.
[24] A. Kitaigorodskii, *Organic Chemical Crystallography*, Consultants Bureau, New York, NY, 1961, pp 106 and 133.